

films and to understand the ablation process and chemical reactivity of ejected species during the plume expansion and propagation.

Acknowledgment. H.-S. Im acknowledges the financial support from Ministry of Science and Technology. This work is supported by the non-directed research fund, the Korea Research Foundation, 1996, which is gratefully acknowledged. We deeply appreciate the efforts of Dr. H. K. Kim in KRISS and Prof. Woo in Chunnam Univ. for preparing the platinized substrates and the helpful discussion of Mr. Y. I. Kim on this work.

References

- Dijkamp, D.; Venkatesan, T.; Wu, X. D.; Sahen, S. A.; Jisrawi, S.; Min-Lee, Y. H.; McLean, W. L.; Croft, M. *Appl. Phys. Lett.* **1987**, *51*, 660.
- Scott, J. F.; Pa de Araujo, C. A. *Science* **1989**, *246*, 1400.
- Krupanidhi, S. B.; Maffei, N.; Sayer, M.; El-Assal, K. J. *Appl. Phys.* **1983**, *54*, 6601.
- Castellano, R. N.; Feinstein, L. G. *J. Appl. Phys.* **1979**, *50*, 4406.
- Okuyama, M.; Togani, Y.; Hamakawa, Y. *Appl. Surf. Sci.* **1988**, *33/34*, 625.
- Payne, D. A. *Bull. Am. Phys. Soc.* **1989**, *34*, 991.
- Otsubo, S.; Maeda, T.; Minamikawa, T.; Yonezawa, Y.; Morimoto, A.; Shimizu, T. *Jpn. J. Appl. Phys.* **1989**, *29*, L133.
- Roy, D.; Kupranidhi, S. B.; Dougherty, J. P. *J. Appl. Phys.* **1991**, *69*, 7930.
- Kidoh, H.; Ogawa, T.; Morimoto, A.; Shimizu, T. *Appl. Phys. Lett.* **1991**, *58*, 2910.
- Ramesh, R.; Luther, K.; Wilkens, B.; Hart, D. L.; Wang, E.; Tarascon, J.; Inam, A.; Wu, X. D.; Venkatesan, T. *Appl. Phys. Lett.* **1990**, *57*, 1505.
- Lee, J.; Safari, A.; Pfeffer, R. L. *Appl. Phys. Lett.* **1992**, *61*, 1643.
- Horwitz, J. S.; Grabowski, K. S.; Chrisey, D. B.; Leuchtner, R. E. *Appl. Phys. Lett.* **1991**, *59*, 1565.
- Ready, J. F. *J. Appl. Phys.* **1965**, *36*, 462.
- Abe, K.; Tomita, H.; Toyoda, H.; Imai, M.; Yokote, Y. *Jpn. J. Appl. Phys.* **1991**, *30*, 2152.
- Amoruso, S.; Berardi, V.; Dente, A.; Spinelli, N.; Armenante, M.; Volott, R.; Fuso, F.; Allegrini, M.; Arimondo, E. *J. Appl. Phys.* **1995**, *78*, 494.
- Masciarelli, G.; Fuso, F.; Allegrini, M.; Arimondo, E. *J. Mol. Spectrosc.* **1992**, *153*, 96.
- Gupta, A. *J. Appl. Phys.* **1993**, *73*, 7877.
- Iembo, A.; Fuso, F.; Allegrini, M.; Arimondo, E.; Berardi, V.; Spinelli, N.; Leccabue, F.; Watts, B. E.; Franco, G.; Chiorboli, G. *Appl. Phys. Lett.* **1993**, *63*, 1194.
- Singh, R. K.; Holland, O. W.; Narayan, J. *J. Appl. Phys.* **1990**, *68*, 223.
- Berardi, V.; Amoruso, S.; Spinelli, N.; Armenante, M.; Velotta, R.; Fuso, F.; Allegrini, M.; Arimondo, E. *J. Appl. Phys.* **1994**, *76*, 8077.
- Singh, R. K.; Narayan, J. *Phys. Rev.* **1990**, *A41*, 8843.
- Kim, H. S.; Kwok, H. S. *Appl. Phys. Lett.* **1992**, *61*, 2234.
- Wu, X. D.; Inam, A.; Venkatesan, T.; Chang, C. C.; Chase, E. W.; Barboux, P.; Tarascon, J. M.; Wilkens, B. *Appl. Phys. Lett.* **1988**, *52*, 752.
- Koren, G.; Gupta, A.; Baseman, R.J.; Lutwyche, M. I.; Laibowitz, R. B. *Appl. Phys. Lett.* **1989**, *55*, 2450.
- Sreenivas, K.; Sayer, M.; Garrett, P. *Thin Solid Films* **1989**, *172*, 251.
- Sayer, M. in *Proceedings of the 6th IEEE International Symposium of Applications of Ferroelectrics*; June 8-11, 1986, Bethlehem, PA, edited by Wood, V. E.; IEEE, New York, 1986; pp 560-568.
- Sreenival, K.; Sayer, M. *J. Appl. Phys.* **1988**, *64*, 1484.

Electrochemical Properties of $\text{Li}_x\text{Co}_y\text{Ni}_{1-y}\text{O}_2$ Prepared by Citrate Sol-Gel Method

Soon Ho Chang, Seong-Gu Kang, and Kee Ho Jang

Electronics and Telecommunications Research Institute, Taejon 305-600, Korea

Received September 6, 1996

The electrochemical properties of $\text{Li}_x\text{Co}_y\text{Ni}_{1-y}\text{O}_2$ compounds ($y=0.1, 0.3, 0.5, 0.7, 1.0$) prepared by citrate sol-gel method have been investigated. The $\text{Li}_x\text{Co}_y\text{Ni}_{1-y}\text{O}_2$ compounds were annealed at 850 °C for 20 h after preheating at 650 °C for 6 h, in air. The x-ray diffraction (XRD) patterns for $\text{Li}_x\text{Co}_y\text{Ni}_{1-y}\text{O}_2$ have shown that these compounds have a well developed layered structure ($R\bar{3}m$). From the scanning electron microscopy of $\text{Li}_x\text{Co}_y\text{Ni}_{1-y}\text{O}_2$, particle size was estimated less than 5 μm . The $\text{Li}/\text{Li}_x\text{Co}_y\text{Ni}_{1-y}\text{O}_2$ electrochemical cell consists of Li metal anode and 1 M LiClO_4 -propylene carbonate (PC) solution as the electrolyte. The differences in intercalation rate of the $\text{Li}_x\text{Co}_y\text{Ni}_{1-y}\text{O}_2$ in the first charge/discharge cycle were less than 0.05 e^- . The first discharge capacities of Li_xCoO_2 and $\text{Li}_x\text{Co}_{0.3}\text{Ni}_{0.7}\text{O}_2$ were ~130 mAh/g and ~160 mAh/g, respectively.

Introduction

LiNiO_2 ,¹⁻⁶ LiCoO_2 ,⁷⁻¹⁵ LiMn_2O_4 ,¹⁶⁻¹⁹ and $\text{Li}_x\text{Co}_y\text{Ni}_{1-y}\text{O}_2$ ²⁰⁻²⁴

have been intensively studied as cathode active materials in lithium secondary batteries. Among them, LiNiO_2 , LiCoO_2 , and $\text{Li}_x\text{Co}_y\text{Ni}_{1-y}\text{O}_2$ are isostructural with $\alpha\text{-NaFeO}_2$. In these

phases; alternate layers of Li and Co (and/or Ni) cations occupy the octahedral site of a cubic close packing of oxygen anions. According to previous studies,^{4,5,22} LiNiO₂ has been nonstoichiometric compound with the formula of [Li⁺_{1-z}Ni²⁺_z][Ni³⁺Ni²⁺]_zO₂ (0 ≤ z ≤ 0.2) depending on preparation conditions. A small amount of structural disorder due to the displacement of nickel and lithium ions in LiNiO₂ strongly affects the electrochemical properties such as the working voltage and rechargeable capacity. As the deintercalation reaction proceeds below x=0.5 in Li_xNiO₂, some structural irreversible rearrangements occur, leading to irreversible electrochemical reactions.² LiCoO₂ is easily prepared and gives a high voltage and a good reversibility in Li/LiMO₂ cells. Although the LiCoO₂ does not have a structural disorder, LiCoO₂ is expensive compare with others and has higher voltage (4 V) than LiNiO₂ (3.5-4.0 V) so that the electrolyte oxidation can be occurred.

These considerations have led to the electrochemical studies of Li_xCo_yNi_{1-y}O₂²⁰⁻²⁴ series. In this study, Li_xCo_yNi_{1-y}O₂ (y=0.1, 0.3, 0.5, 1.0) system synthesized by citrate sol-gel method has been investigated. The structure and electrochemical properties of the Li_xCo_yNi_{1-y}O₂ have been evaluated and compared with those of Li_xCo_yNi_{1-y}O₂ prepared by solid state reaction.

Experimental

Li_xCo_yNi_{1-y}O₂ (y=0.1, 0.3, 0.5, 1.0) compounds were prepared by citrate sol-gel method (Li_xCo_yNi_{1-y}O₂(C)) and conventional solid state reaction (Li_xCo_yNi_{1-y}O₂(S)). The Li_xCo_yNi_{1-y}O₂(C) (y=0.1, 0.3, 0.5, 1.0) were obtained by using citric acid (C₆H₈O₇) as follows; Li₂CO₃, Co(NO₃)₂·6H₂O, Ni(NO₃)₂·6H₂O, and C₆H₈O₇ were dissolved with the mole ratio of 1 : y : (1-y) : 3 in distilled water. The solution was adjusted to pH=3-4 with aq. NH₄OH by considering solubility diagram. The solution was evaporated at 80 °C under vacuum and the subsequent organometallic complexes were decomposed into organic compounds and metal oxide precursor at 300 °C. The metal oxide precursor was pre-heated at 600 °C for 6 h and annealed at 850 °C for 20 h, in air to obtain Li_xCo_yNi_{1-y}O₂(C) compounds. The synthesis of Li_xCo_yNi_{1-y}O₂(S) (y=0.1, 0.3, 0.5, 1.0) with solid state reaction has already been reported.²⁴ It consists of heating a mixture of Li₂CO₃, CoCO₃ and NiO, in appropriate ratio, at 800-1000 °C for 48 h in air after preheating 650 °C for 10 h, in air.

Structural analysis has been performed by x-ray diffractometer (Rigaku RTP 300 RC) with Ni-filtered Cu-Kα radiation (λ=1.5418 Å). Scanning electron microscopy have been recorded by Hitachi S800 microscope in order to investigate the morphology of Li_xCo_yNi_{1-y}O₂.

The electrochemical cell was fabricated as follows. A cathode was made 89% (wt.%) Li_xCo_yNi_{1-y}O₂, 10% acetylene black, and 1% PTFE binder. The electrolyte used was 1 M LiClO₄-propylene carbonate (PC) solution. A lithium metal anode was used in this study. Test cell were assembled in a glove box filled with argon. The cells were cycled in the voltage range 3.0-4.1 V with various current densities using galvanostatic charge/discharge cycle.

Results and Discussion

The x-ray diffraction (XRD) patterns for Li_xCo_yNi_{1-y}O₂ obtained by citrate sol-gel method and conventional solid state reaction have been indexed with hexagonal symmetry. Lattice parameters of the Li_xCo_yNi_{1-y}O₂(C), which were obtained from least squares method, and c/a ratio are presented in Table 1. The a and c parameters, related to the intralayer metal-metal distance and interslab distance respectively, decrease with increasing cobalt concentration in Li_xCo_yNi_{1-y}O₂(C) due to the difference in size between the trivalent cobalt (r(Co³⁺)=0.53 Å, low spin (t_{2g}⁶e_g⁰) and nickel (r(Ni³⁺)=0.56 Å, low spin (t_{2g}⁶e_g¹) ions. The c/a ratio, indicating the structure anisotropy of Li_xCo_yNi_{1-y}O₂(C), increases when Co³⁺ is substituted for nickel (c/a=2√6 for a cubic lattice). This variation indicates that the 2D character is increased with substituting cobalt for nickel ions. The results of structural analysis for Li_xCo_yNi_{1-y}O₂(S) are similar

Table 1. Structural parameters of Li_xCo_yNi_{1-y}O₂(R $\bar{3}$ m)

y	a (Å)	c (Å)	c/a
0.1	2.877	14.17	4.925
0.3	2.860	14.15	4.948
0.5	2.844	14.11	4.961
0.7	2.833	14.10	4.977
0.9	2.821	14.07	4.987
1	2.814	14.04	4.989

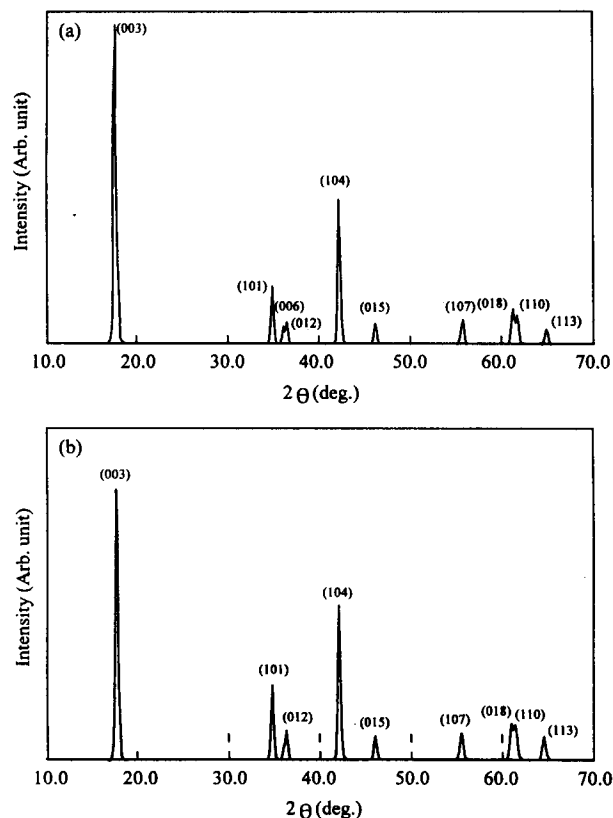


Figure 1. X-ray powder diffraction patterns for (a) LiCo_{0.3}Ni_{0.7}O₂(C) and (b) LiCo_{0.3}Ni_{0.7}O₂(S).

to those of $\text{Li}_x\text{Co}_y\text{Ni}_{1-y}\text{O}_2(\text{C})$.

The XRD pattern for $\text{Li}_x\text{Co}_y\text{Ni}_{1-y}\text{O}_2(\text{C})$ ($y=0.3$) shows good splitting of (006) and (012), and (018) and (110) lines (Figure 1(a)). However, $\text{Li}_x\text{Co}_y\text{Ni}_{1-y}\text{O}_2(\text{S})$ ($y=0.3$) has no (012) line and the split of (108) and (110) lines can be slightly observed (Figure 1(b)). This indicates that the compounds prepared by using citric acid have better crystallinity than those by conventional method. The results of XRD analysis for $\text{Li}_x\text{Co}_y\text{Ni}_{1-y}\text{O}_2$ ($y=0.3$) are given in Table 2. As shown in Table 2, the relative intensity of (003) with citrate method was higher than that with solid state one. In the LiMO_2 ($M=\text{V}, \text{Cr}, \text{Co}, \text{Fe}, \text{Ni}$) phase, alternate layers of Li and M cations occupy the octahedral site of a compact cubic close packing of oxide anions as previously mentioned.²⁵ When M atoms occupy parts of the octahedral sites of the Li layer, the (003) line intensity decreases. Thus, the strong intensity of (003) line for $\text{Li}_x\text{Co}_y\text{Ni}_{1-y}\text{O}_2$ indicates that the $\text{Li}_x\text{Co}_y\text{Ni}_{1-y}\text{O}_2$ have strongly enhanced 2D character. The scanning electron microscopy of $\text{LiCoO}_2(\text{C})$ exhibits that the compound with citrate method has a well developed layered structure and its particle size is less than 5 μm (Figure 2). The particle size of $\text{LiCoO}_2(\text{C})$ is smaller than that of $\text{LiCoO}_2(\text{S})$ ($\leq 10 \mu\text{m}$).

The charge/discharge behavior in the first cycle for Li/ $\text{Li}_x\text{Co}_y\text{Ni}_{1-y}\text{O}_2$ cell using the $\text{Li}_x\text{Co}_y\text{Ni}_{1-y}\text{O}_2$ obtained from ci-

trate organometallic complex and solid state reaction was examined under constant current density (200 $\mu\text{A}/\text{cm}^2$). Figure 3 shows the first cycle of voltage vs. x . The differences of intercalation rate(x) between charge and discharge for $\text{Li}_x\text{Co}_y\text{Ni}_{1-y}\text{O}_2(\text{C})$ and $\text{Li}_x\text{Co}_y\text{Ni}_{1-y}\text{O}_2(\text{S})$ are $\sim 0.05 e^-$ and $\sim 0.09 e^-$, respectively. This implies that the $\text{Li}_x\text{Co}_y\text{Ni}_{1-y}\text{O}_2(\text{C})$ has smaller irreversible loss and better reversibility of electrochemical reaction compared with $\text{Li}_x\text{Co}_y\text{Ni}_{1-y}\text{O}_2(\text{S})$. The first discharge capacities of Li_xCoO_2 and $\text{Li}_x\text{Co}_{0.3}\text{Ni}_{0.7}\text{O}_2$ by citrate method are $\sim 130 \text{mAh/g}$ and $\sim 160 \text{mAh/g}$, respectively. These values are higher than those by solid state reaction ($\sim 120 \text{mAh/g}$ and $\sim 140 \text{mAh/g}$, respectively). The charge/discharge behavior of $\text{Li}_x\text{Co}_y\text{Ni}_{1-y}\text{O}_2(\text{C})$ shows that the best cycling properties were observed in the Li/Li_xCo_{0.3}Ni_{0.7}O₂(C) cell. This behavior means that any structural disorder due to the displacement of nickel (and/or cobalt) and lithium ions in the $\text{Li}_x\text{Co}_{0.3}\text{Ni}_{0.7}\text{O}_2(\text{C})$ is not appeared.

In order to examine the current dependency of Li/Li_xCo_{0.3}Ni_{0.7}O₂(C) cell, the cell has been cycled at various current densities (Figure 4). As the current density increases from 200 $\mu\text{A}/\text{cm}^2$ to 500 $\mu\text{A}/\text{cm}^2$, the changes of capacity and cell polarization were small. The reversibility has been hardly affected even under a high current density. These phenomena proved that the compound obtained by citrate sol-gel method is structurally stable during the electrochemical reaction.

Figure 5 shows the charge and discharge curves of the Li/Li_xCoO₂(C) cell at a current density of 200 $\mu\text{A}/\text{cm}^2$. The current was automatically switched on for 6 h and off for 20 h. The difference of open circuit voltage between decreasing and increasing x in the $\text{Li}_x\text{CoO}_2(\text{C})$, related to cell polarization, is very small. This indicates that the lithium diffusion in the interslab of the $\text{Li}_x\text{CoO}_2(\text{C})$ is readily occurred due to the small particle size of the compound.

The XRD analysis for the $\text{Li}_x\text{Co}_{0.3}\text{Ni}_{0.7}\text{O}_2(\text{C})$ with various Li concentration ($x=0.6, 0.7, 0.8, 0.9, 1.0$) was carried out to investigate the structural change during the electrochemical oxidation (Table 3, Figure 6). The XRD patterns show that crystallinity of $\text{Li}_x\text{Co}_{0.3}\text{Ni}_{0.7}\text{O}_2(\text{C})$ is well maintained during the electrochemical deintercalation. This implies that 2D structure of the $\text{Li}_x\text{Co}_y\text{Ni}_{1-y}\text{O}_2(\text{C})$ is preserved during the elimination of Li atoms. The decrease in the a

Table 2. Structural analysis of $\text{Li}_x\text{Co}_y\text{Ni}_{1-y}\text{O}_2$ ($y=0.3$) ($a=2.860 \text{ \AA}$, $c=14.15 \text{ \AA}$ in hexagonal cell)

(hkl)	d_{obs}^*	d_{obs}	d_{cal}	I_{obs}^*	I_{obs}	I_{cal}
(003)	4.726	4.726	4.718	100	100	100
(101)	2.441	2.441	2.439	15	28	39
(006)	2.356		2.359	5	0	4
(012)	2.337	2.339	2.337	6	11	12
(104)	2.029	2.030	2.029	37	57	79
(105)	1.865	1.864	1.864	6	9	12
(107)	1.566	1.567	1.566	7	10	14
(018)	1.439	1.439	1.439	10	13	19
(110)	1.430	1.430	1.430	8	13	20
(113)	1.368	1.368	1.368	4	8	13

d_{obs}^* , I_{obs}^* : citrate sol-gel method, d_{obs} , I_{obs} : solid state reaction

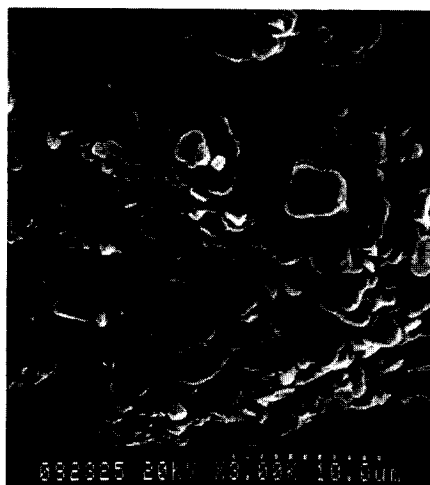


Figure 2. Scanning electron microscopy of $\text{LiCoO}_2(\text{C})$.

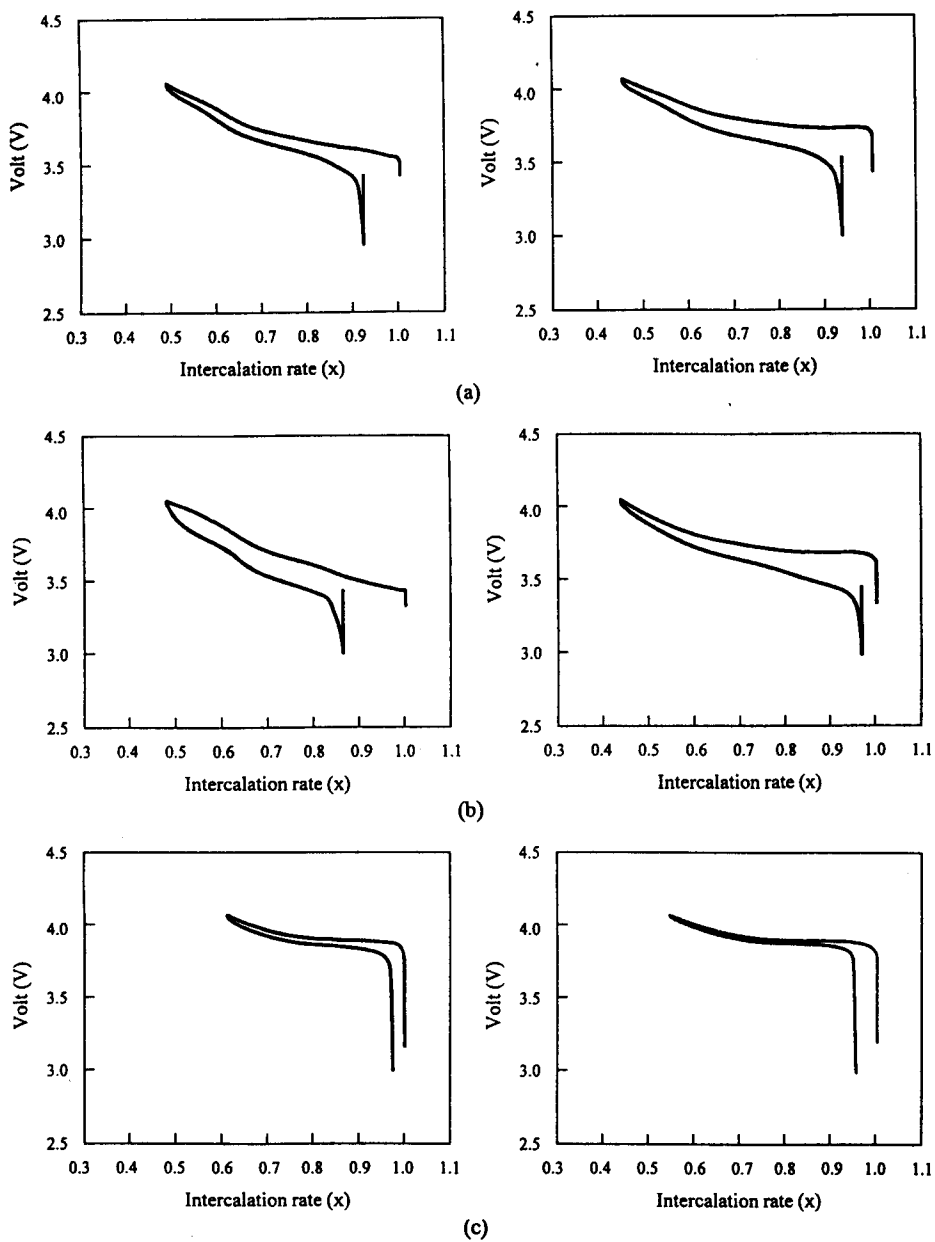


Figure 3. First charge and discharge curves of $\text{Li}/\text{Li}_x\text{Co}_y\text{Ni}_{1-y}\text{O}_2(\text{C})$ and $\text{Li}/\text{Li}_x\text{Co}_y\text{Ni}_{1-y}\text{O}_2(\text{S})$ with (a) $y=0.1$, (b) 0.3 , and (c) 1.0 , respectively at constant current density ($200 \mu\text{A}/\text{cm}^2$).

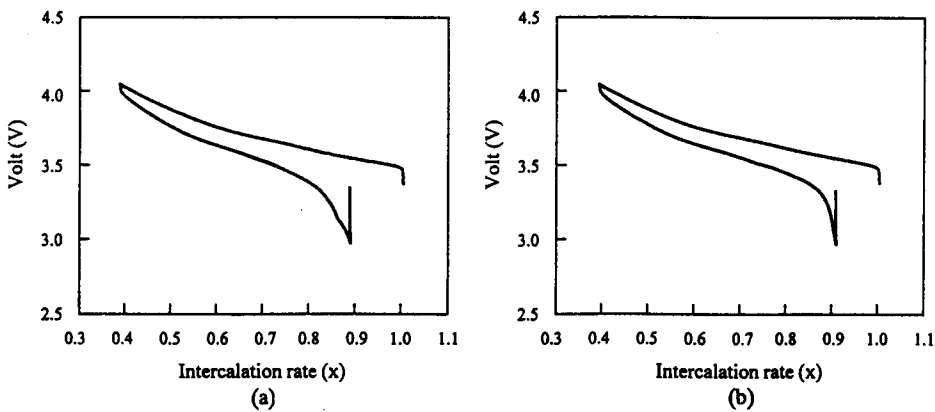


Figure 4. The current dependency of $\text{Li}/\text{Li}_x\text{Co}_{0.3}\text{Ni}_{0.7}\text{O}_2(\text{C})$ cell. (a) $300 \mu\text{A}/\text{cm}^2$. (b) $500 \mu\text{A}/\text{cm}^2$.

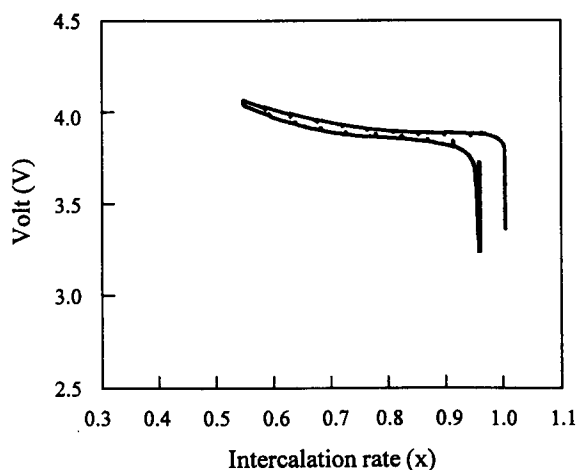


Figure 5. Charge and discharge curves of $\text{Li}/\text{Li}_x\text{Co}_y\text{Ni}_{1-y}\text{O}_2(\text{C})$ cell with relaxation (current density = $200 \mu\text{A}/\text{cm}^2$).

Table 3. Variation of structural parameters for $\text{Li}_x\text{Co}_y\text{Ni}_{1-y}\text{O}_2$ ($y=0.3$) with various Li concentration ($x=0.6, 0.7, 0.8, 0.9, 1.0$)

x	a	c	c/a
1.0	2.860	14.15	4.948
0.9	2.855	14.18	4.967
0.8	2.847	14.22	4.994
0.7	2.836	14.28	5.035
0.6	2.827	14.32	5.065

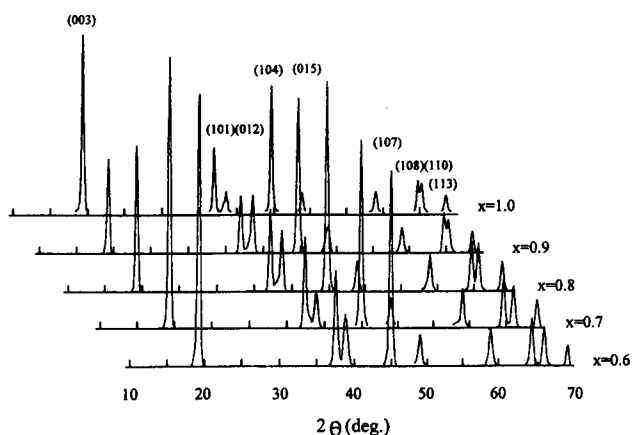


Figure 6. X-ray powder diffraction patterns for $\text{Li}_x\text{Co}_{0.3}\text{Ni}_{0.7}\text{O}_2(\text{C})$ with various Li concentration ($x=0.6, 0.7, 0.8, 0.9, 1.0$).

parameter with decreasing Li^+ ion concentration (x) of $\text{Li}_x\text{Co}_y\text{Ni}_{1-y}\text{O}_2(\text{C})$ reflects the decrease in Li^+-Li^+ electrostatic repulsion within a basal plane. The c -axis of the $\text{Li}_x\text{Co}_y\text{Ni}_{1-y}\text{O}_2(\text{C})$ expands rapidly upon delithiation due to the decrease of electrostatic binding energy of the lithium-depleted layers.

Conclusion

$\text{Li}_x\text{Co}_y\text{Ni}_{1-y}\text{O}_2$ compounds were successfully prepared by citrate sol-gel method. The obtained $\text{Li}_x\text{Co}_y\text{Ni}_{1-y}\text{O}_2$ exhibit well developed layered structure and were structurally stable during the electrochemical reaction. The $\text{Li}_x\text{Co}_y\text{Ni}_{1-y}\text{O}_2$

are smaller irreversible loss and better reversibility of electrochemical reaction compared with $\text{Li}_x\text{Co}_y\text{Ni}_{1-y}\text{O}_2$ prepared by solid state reaction. The first discharge capacities of the $\text{Li}_x\text{Co}_y\text{Ni}_{1-y}\text{O}_2$ are higher and the changes of capacity and cell polarization are smaller than those by solid state reaction.

References

- Dahn, J. R.; Sacken, U. von; Michal, C. A. *Solid State Ionics* **1990**, *44*, 87.
- Morales, J.; Perez-Vicente, C.; Tirado, J. L. *Mat. Res. Bull.* **1990**, *25*, 623.
- Ohzuku, T.; Ueda, A.; Nagayama, M. *J. Electrochem Soc.* **1993**, *140*, 1862.
- Dutta, G.; Manthiram, A.; Goodenough, J. B.; Grenier, J. C. *J. Solid State Chem.* **1992**, *96*, 123.
- Rougier, A.; Delmas, C.; Chadwick, A. V. *Solid State Comm.* **1995**, *94*, 123.
- Dahn, J. R.; Sacken, U. von; Juzkow, M. W.; Al-Janaby, H. *J. Electrochem Soc.* **1991**, *138*, 2207.
- Mizushima, K.; Jones, P. C.; Wiseman, P. J.; Goodenough, J. B. *Mat. Res. Bull.* **1980**, *15*, 783.
- Delmas, C.; Braconnier, J. J.; Hagenmuller, P. *Mat. Res. Bull.* **1982**, *17*, 117.
- Plichta, E.; Salomon, M.; Slane, S.; Uchiyama, M. *J. Power Sources* **1987**, *21*, 25.
- Plichta, E.; Slane, S.; Uchiyama, M.; Salomon, M.; Chua, D.; Ebner, W. B.; Lin, H. W. *J. Electrochem Soc.* **1989**, *136*, 1865.
- Dahn, J. R.; Reimers, J. N. *J. Electrochem Soc.* **1992**, *139*, 2091.
- Dahn, J. R.; Reimers, J. N.; Sacken, U. von, *J. Electrochem Soc.* **1992**, *140*, 2752.
- Ohzuku, T.; Ueda, A. *J. Electrochem Soc.* **1994**, *141*, 2972.
- Bludska, J.; Vondrak, J.; Stopka, P.; Jakubec, I. *J. Power Sources* **1992**, *39*, 313.
- Yoshio, M.; Tanaka, H.; Tominaga, K.; Noguchi, H. *J. Power Sources* **1992**, *40*, 347.
- Barboux, P.; Tarascon, J. M.; Shokoohi, F. K. *J. Solid State Chem.* **1991**, *94*, 185.
- Guyomard, D.; Tarascon, J. M. *Solid State Ionics* **1994**, *69*, 222.
- Zachau-Christiansen, B.; West, K.; Jacobsen; Skaarup, S. *Solid State Ionics* **1994**, *70/71*, 401.
- Richard, M. N.; Fuller, E. W.; Dahn, J. R. *Solid State Ionics* **1994**, *73*, 81.
- Delmas, C.; Saadoune, I. *Solid State Ionics* **1992**, *53-56*, 370.
- Delmas, C.; Saadoune, I.; Rougier, A. *J. Power Sources* **1993**, *43-44*, 595.
- Zhecheva, E.; Stoyanova, R. *Solid State Ionics* **1993**, *66*, 143.
- Ueda, A.; Ohzuku, T. *J. Electrochem Soc.* **1994**, *141*, 2010.
- Menetrier, M.; Rougier, A.; Delmas, C. *Solid State Comm.* **1994**, *90*, 439.
- Hewston, T. A.; Chamberland, B. L. *J. Phys. Chem. Solids* **1987**, *48*, 97.